Simulating photons and plasmons in a three-dimensional lattice

A. Pletzer [a], and G. Shvets [b]

[a] *Princeton Plasma Physics Laboratory*
PO Box 451
Princeton NJ 08543

[b] *Illinois Institute of Technology*
3101 South Dearborn
Chicago, IL 60616

Abstract

Three-dimensional metallic photonic structures are studied using a newly developed mixed finite element-finite difference (FE-FD) code, Curly3d. The code solves the vector Helmholtz equation as an eigenvalue problem in the unit cell of a triply periodic lattice composed of conductors and/or dielectrics. The mixed FE-FD discretization scheme ensures rapid numerical convergence of the eigenvalue and allows the code to run at low resolution. Plasmon and photonic band structure calculations are presented.

Key words: Band structure, Helmholtz equation, 3-D, mixed FE-FD, perfect conductor

1 Background

The recent upsurge of interest in the electrodynamics of three-dimensional periodic structures is due to the realization that composite materials can exhibit unusual electromagnetic properties. For example, a composite material made of poles and split ring-resonators can display negative dielectric permittivity and magnetic permeability for a range of frequencies [1]. Such materials known

[1] This work supported by the U.S. Department of Energy under DE-AC02-76CH03073.

as left-handed materials support electromagnetic waves with a very counter-intuitive behavior: their group and phase velocities oppose each other. Left-handed materials can be used for developing, for example, "perfect" lenses [2] capable of sub-wavelength resolution.

Key to understanding the bulk properties of the infinitely extended composite materials is the accurate determination of the band structure of the electromagnetic waves by solving Maxwell's equations. In the frequency domain, the wave equation becomes

$$\boldsymbol{\nabla}\times\left(\mu^{-1}\cdot\boldsymbol{\nabla}\times\mathbf{E}\right)=\frac{\omega^2}{c^2}\epsilon\cdot\mathbf{E} \tag{1}$$

where $\mathbf{E}$ is the electric field and μ (ϵ) the permeability (permittivity) of the medium. Both ϵ and μ are spatially varying tensors. The perfect conductor boundary condition $\mathbf{E}\times\mathbf{n}=0$, where $\mathbf{n}$ is the normal, is applied at the conductor boundaries. Because of the system periodicity, and according to Floquet's theorem, the electric field can be expressed as $\tilde{\mathbf{E}}\exp\mathrm{i}\mathbf{k}\cdot\mathbf{x}$, where $\tilde{\mathbf{E}}(\mathbf{x}+\mathbf{L})=\tilde{\mathbf{E}}(\mathbf{x})$ is a periodic function, $\mathbf{L}$ is any one of the periodicity vectors, and $\mathbf{k}$ is inside the Brillouin zone. Therefore, it is sufficient to solve Eq. (1) inside the unit cell, which we assume to be a parallelepiped with the dimensions $L_x\times L_y\times L_z$. The equation for $\tilde{\mathbf{E}}$ can be obtained from (1) by replacing $\boldsymbol{\nabla}$ by $\boldsymbol{\nabla}+\mathrm{i}\mathbf{k}$:

$$(\boldsymbol{\nabla}+\mathrm{i}\mathbf{k})\times\left[\mu^{-1}\cdot(\boldsymbol{\nabla}+\mathrm{i}\mathbf{k})\times\tilde{\mathbf{E}}\right]=\frac{\omega^2}{c^2}\epsilon\cdot\tilde{\mathbf{E}}. \tag{2}$$

Here, $\mathbf{k}\cdot\mathbf{L}$ represents, up to a term $2\pi(m+n+l)$ (m,n and l are integers), the phase shift experienced by the wave across the unit cell. For $m=n=l=0$, $\mathbf{k}$ can be thought of as the wave vector of an incident wave. From now on we will focus on $\tilde{\mathbf{E}}$ and drop the $\tilde{}$ for notational simplicity.

Note that we have chosen here to write the equation for $\mathbf{E}$. The equation for the magnetic field $\mathbf{H}$ is similar to (2) except for ϵ and μ playing opposite roles. Hence, the pairs $(\epsilon,\mathbf{E})$ and $(\mu^\dagger,\mathbf{H}^*)$ can be regarded as dual of each other (the complex * and Hermitian † conjugates are required to derive the Poynting flux involving $\mathbf{E}$ only from an expression solely based on $\mathbf{H}$ and vice-versa). This duality extends to the jump conditions across permittivity discontinuities ($[[\mathbf{n}\cdot\epsilon\cdot\mathbf{E}]]=0$) and permeability discontinuities ($[[\mathbf{n}\cdot\mu\cdot\mathbf{H}]]=0$) but *not*, however, to the boundary conditions at the surface of perfect conductors. While the tangential $\mathbf{E}$ ($\mathbf{E}_t$) must be set to zero there, it is the *normal* component of $\mathbf{H}$ (H_n) that is required to vanish at the conductor so that the mode structure of magnetic and electric fields will in general to be fundamentally different. It turns out that solving for $\mathbf{H}$ is from a coding viewpoint straightforward because $H_n=0$ are the default (homogeneous natural) boundary conditions of

the FE method. On the other hand, solving for $\mathbf{E}$ involves applying (explicit) Dirichlet conditions, which turns out to be numerically more efficient.

2 Discretization

In order to solve (2), the field (e.g. electric) is expanded $\mathbf{E} = \sum_j E_j \mathbf{e}_j(\mathbf{x})$ in finite vector elements $\mathbf{e}_j$. Our choice of $\mathbf{e}_j$'s is motivated by the desire to capture accurately discontinuities at conductor and dielectric interfaces. Van Welij elements [3], by being piecewise linear in the directions perpendicular to the field *but* only piecewise continuous along the field, are well suited for this purpose. Such a spatial dependence ensures that each $\mathbf{e}_j$ is divergence-free within an elemental mesh unit. Van Welij elements do not appear to suffer from numerical pollution (spurious modes) [4], a problem that commonly afflicts other types of discretizations. However, van Welij elements require a rectilinear mesh. Although later generalized to curvilinear meshes [5], we found that using straight hexahedral (brick) elements has a number of advantages not least that the domain can be built incrementally. Each brick can be identified by a triplet (i, j, k), $i = 1, \cdots N_x$, $j = 1, \cdots N_y$ and $k = 1, \cdots N_z$. Complex geometries can thus be constructed by adding and removing bricks at will, while noting that doing so has the disadvantage of introducing "staircase" interfaces.

The discretized version of the vector Helmholtz equation is obtained after multiplying (2) by a test function $\mathbf{e}_i$, integrating over the unit cell domain and applying the divergence theorem to yield the generalized eigenvalue system

$$\sum_j A_{ij} E_j = \lambda \sum_j B_{ij} E_j \tag{3}$$

where the eigenvalue is $\lambda \equiv \omega^2/c^2$,

$$A_{ij} = \int dV (\boldsymbol{\nabla} + \mathrm{i}\mathbf{k})^* \times \mathbf{e}_i \cdot \mu^{-1} \cdot (\boldsymbol{\nabla} + \mathrm{i}\mathbf{k}) \times \mathbf{e}_j \tag{4}$$

and

$$B_{ij} = \int dV \mathbf{e}_i \cdot \epsilon \cdot \mathbf{e}_j \tag{5}$$

are two sparse matrices and integration is over the volume of the unit cell. To be exact, the integration by parts introduces a surface term $\oint d\boldsymbol{\sigma} \cdot \mathbf{e}_i \times [\mu^{-1} \cdot (\boldsymbol{\nabla} + \mathrm{i}\mathbf{k}) \times \mathbf{E}]$ in the left-hand side of (3). But by virtue of $\mathbf{E}$ being periodic this term does not contribute on unit cell faces. Nor does it contribute on perfect conductor faces since $\mathbf{E}_t = 0$ there. Finally, it is straightforward to see that this

term also cancels at conductor faces when solving for $\mathbf{H}$ (replace $\mu \to \epsilon$ and $\mathbf{E} \to \mathbf{H}$ in the above) since we have $(\epsilon^{-1} \cdot [\boldsymbol{\nabla} + \mathrm{i}\mathbf{k}] \times \mathbf{H})_t \sim \mathbf{E}_t = 0$.

So far we have not deviated from a standard implementation of the FE method. Integrals (4) and and (5) can be computed analytically assuming ϵ and μ to be constant in each brick, with the matrix A yielding a stencil approximation of operator $(\boldsymbol{\nabla} + \mathrm{i}\mathbf{k}) \times \mu^{-1} \cdot (\boldsymbol{\nabla} + \mathrm{i}\mathbf{k}) \times$ and matrix B an approximation to ϵ. When $\epsilon = 1$, the B-stencil for parallel edges

$$\begin{array}{ccccc} \frac{1}{36} & & \frac{1}{9} & & \frac{1}{36} \\ & & \uparrow & & \\ \frac{1}{9} & \longleftarrow & \frac{4}{9} & \longrightarrow & \frac{1}{9} \\ & & \downarrow & & \\ \frac{1}{36} & & \frac{1}{9} & & \frac{1}{36} \end{array} \tag{6}$$

can be regarded as a crude approximation of the identity operator. Had we chosen an FD approach, then the coefficient $\frac{4}{9}$ would have been 1 with all other coefficients set to zero. This suggests that a certain degree of freedom is available in the choice of B-stencil. It can be shown that this choice in B-stencil does not compromise the uniqueness of the solution. Rather, it reflects the fact that the numerical error is dominated in the FE method by the A-stencil at high resolution with modifications of B allowed provided they are of same or higher order of accuracy. This degree of freedom is therefore similar to the choice of quadrature method in the tunable integration scheme of Bondeson and Fu [6], and the motivation in Curly3d for introducing a free parameter Δ, which allows for some flexibility in the choice of B-stencil

$$\begin{array}{ccccc} 0 & & \frac{1-\Delta}{2} & & 0 \\ & & \uparrow & & \\ \frac{1-\Delta}{2} & \longleftarrow & 2\Delta - 1 & \longrightarrow & \frac{1-\Delta}{2} \\ & & \downarrow & & \\ 0 & & \frac{1-\Delta}{2} & & 0 \end{array} . \tag{7}$$

When Δ is set to 1 we recover the FD stencil while $\Delta = 2/3$ gives approximately the FE stencil. Choosing the appropriate value of Δ so as to minimize the error is the subject of the following section.

3 Results

We now test the numerical convergence of the mixed FE-FD scheme by first considering a structure made of perfectly conducting (metallic) cubes of size $\frac{a}{2}\times\frac{a}{2}\times\frac{a}{2}$ embedded in an $\epsilon = \mu = 1$ material. The cubes, which form a periodic structure, are separated by distance a, the periodicity length. We reproduce here the results of Mias et al. [7] in Section 4.4 of their paper.

Figure 1 (a) shows the second Brillouin zone (the first Brillouin zone which contains the point $\omega = 0$ at $\mathbf{k} = 0$ is not shown). The solid line was obtained by solving the equation for $\mathbf{E}$ and using 16 bricks along each direction, whereas all other curves were obtained at low 8^3 resolution. The high resolution dispersion curve is in good agreement with the upper band shown in Fig. 12 of Ref. [7]. Due to the variational nature of the FE discretization, it is apparent that the FE method systematically overestimates the eigenfrequency. In contrast, the FD discretization tends to underestimate the eigenfrequency. The mixed FE-FD scheme is found to perform best when solving for $\mathbf{H}$. We chose a value $\Delta = 5/6$, which can be shown to be optimal for plane waves. Despite the departure of the solution from the a plane wave due to scattering occurring at the conductors, the value $\Delta = 5/6$ can be seen to yield an accuracy that is comparable to the one achieved at higher 16^3 resolution using the standard FE method, an impressive result considering the fact that the 16^3 case takes 50 times longer to run.

Having shown that a single Δ can improve the accuracy over a wide range of $\mathbf{k}$ values, we now investigate the effect of the mode polarization on the convergence properties by considering a lattice of intersecting conducting rods, which are immersed in an $\epsilon = \mu = 1$ medium. Such a geometry has recently attracted interest as a possible means to fabricate media with negative permittivity [8]. Each conductor of cross-section $\frac{a}{3}\times\frac{a}{3}$ is aligned to the principal axes of the $a\times a\times a$ cell. In contrast to the previous test case, such a structure exhibits a cutoff frequency [c.f. Fig. 1 (b)]. In the neighborhood of $\mathbf{k} = 0$ (point Γ in reciprocal space) two photonic and one plasmon branches emerge with the plasmon eigenvalue $\omega^2 a^2/(2\pi c)^2$ having a weaker dependence in $|\mathbf{k}|^2$. At $\mathbf{k}a/(2\pi) = (0.2, 0, 0.3)$, however, we found the plasmon to have eigenvalue $\omega^2 a^2/(2\pi c)^2 = 0.352$, that is only slightly below the two photonic branches 0.386 and 0.408, respectively. Analysis of the mode structure revealed the plasmon's field to be predominantly aligned to $\mathbf{k}$. In contrast, the two photon fields are oriented mainly perpendicular to $\mathbf{k}$. In spite of the difference in their mode structures, we find in Fig. 2 that the convergence rate can be significantly improved for both types of modes by selecting a single mixture parameter Δ between 0.8 and 1.

We now test the capability of Curly3d to handle both positive and *negative*

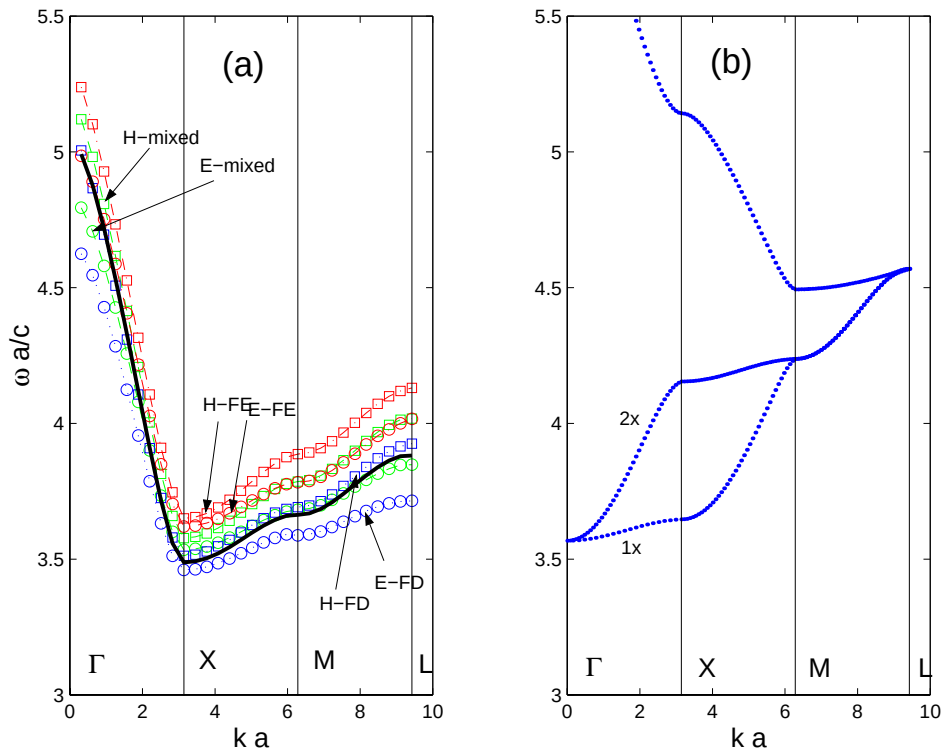

Fig. 1. Dispersion curves obtained by marching in reciprocal space from [000] → [100] → [110] → [111]. (a) Metallic cavity of size $a/2$: the curves emphasizing the accuracy of the mixed FE-FD scheme were obtained at low 8^3-resolution by solving for $\mathbf{E}$ (circles) and $\mathbf{H}$ (squares) and using three mixture parameters Δ. For reference, the solid curve was obtained using the FE scheme at 16^3-resolution. (b) Dispersion curves for the geometry of intersecting conductors with cutoff at $\omega a/c \approx 3.6$.

ϵ and μ. Materials with negative ϵ in a narrow frequency range occur in nature. They include polar crystals (ZnSe, SiC) and free electron plasmas. The geometry is that of a cubic $\frac{a}{2}\times\frac{a}{2}\times\frac{a}{2}$ insertion of a dielectric with negative permittivity (permeability). Here, we solved for the electric field and kept $\mathbf{k}a/(2\pi) = (0.5, 0, 0)$ fixed while decreasing ϵ (μ) from 1 to a -1.1. In the process, the eigensolution at each step was fed to an inverse iteration eigensolver as initial guess to the next step. The eigenfrequency as a function of ϵ is plotted in Fig. 3. For $\epsilon = \mu = 1$, the solution is a plane wave with the numerical eigenfrequency converging to the exact value to within machine accuracy. As ϵ approaches zero, the electric field becomes increasingly tangential to the dielectric surface and a surface mode develops. The eigenfrequency is ill-defined at $\epsilon = 0$. Nonetheless, the mode can be accurately tracked across this point and the eigenfrequency calculation pursued in the negative ϵ regime. As ϵ further decreases, sharp features arise at the interface due to the rapid decay of the wave in the negative dielectric, with the normal electric field flipping sign at the surface. This is also a regime where it becomes increasingly difficult to track the mode as the spectrum becomes denser with new modes emerging from below. Varying μ instead of ϵ produces a similar curve except for mode

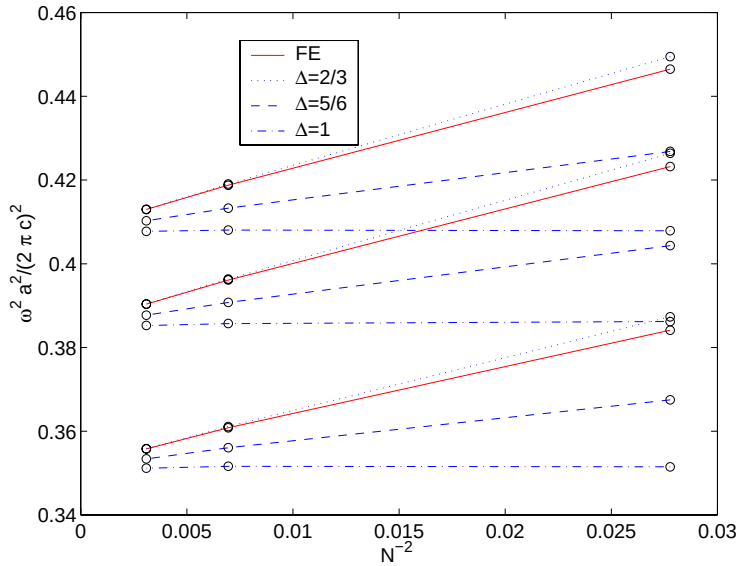

Fig. 2. Convergence of the eigenvalue λ in the number $N = N_x = N_y = N_z$ of bricks for the plasmon and photonic modes with conducting rods of size $\frac{a}{3}\times\frac{a}{3}$, $a = 2\pi$, and $\mathbf{k} = (0.2, 0, 0.3)$.

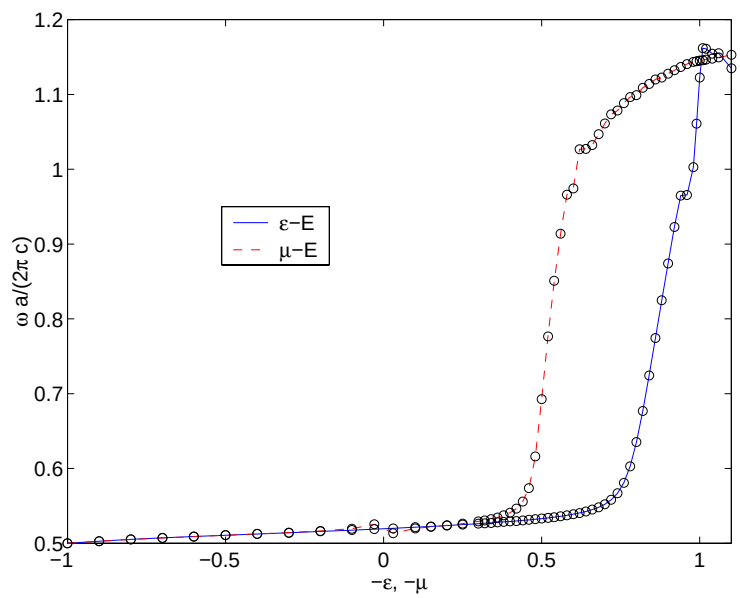

Fig. 3. Dependence of the eigenfrequency on the permittivity (solid line) and permeability (dashed line) inside a cubic of size $\frac{a}{2}\times\frac{a}{2}\times\frac{a}{2}$. Results obtained using 12^3 elements and $\Delta = 1$.

conversion occurring in the negative regime. Agreement between the ϵ-$\mathbf{E}$ and μ-$\mathbf{E}$ curves is expected since, by virtue of the duality principle, the equations for (μ, $\mathbf{E}$) and (ϵ, $\mathbf{H}$) are indistinguishable. We have tested that individual points on the $\epsilon < -0.4$ branch of the ϵ-$\mathbf{E}$ curve can also be obtained by running in μ-$\mathbf{E}$ mode and vice versa so that the appearance of two branches can be explained in terms of coupling to neighboring modes.

4 Conclusions

We have presented a code, Curly3d, designed for the calculations of band structures in metallic and dielectric crystals. Curly3d differs from the MIT Photonic-Band code [9] in that the crystal can have embedded conductors as well as a spatially varying permeability.

Curly3d uses a mixed finite element, finite difference scheme to accelerate the numerical convergence of the eigenvalue calculation. By appropriately tuning the mixing parameter Δ we were able to show that the accuracy of the numerical results can be improved so as to enable one to run, typically, at half the resolution required by the finite element method. Moreover, the mixing parameter Δ does not depend sensitively on the wave-vector or on the mode polarization.

A large part of Curly3d, including the matrix assembly, is written in the scripting language Python thus making it easy for users to extend the code. Extensive use of nested lists, hash tables and other advanced data types were made in order to map data on unstructured meshes, composed in our case of uniform bricks. Curly3d relies on the Ellipt2d package [10]. Both Ellipt2d and Curly3d are freely available and can be downloaded from the CVS repository at `http://sourceforge.net`.

References

[1] D. R. Smith, W. J. Padilla, D. C. Vier, S. C. Nemat-Nasser, S. Schultz, Composite medium with simultaneously negative permeability and permittivity, Phys. Rev. Letters 84 (2000) 4184.

[2] J. B. Pendry, Negative refraction makes a perfect lens, Phys. Rev. Lett. 85 (2000) 3966.

[3] J. S. van Welij, Calculation of eddy currents in terms of h on hexahedra, IEEE Transactions on Magnetics 21 (1985) 2239.

[4] P. P. Silvester, R. L. Ferrari, Finite Elements for Electrical Engineers, Cambridge University Press, 1996, Ch. 7, pp. 312–316.

[5] C. W. Crowley, P. P. Silvester, H. Hurwitz, Covariant projection elements for 3d vector field problems, IEEE Transactions on Magnetics MAG-18 (1988) 431.

[6] A. Bondeson, G. Y. Fu, Tunable integration scheme for the finite element method, Comput. Phys. Commun. 66 (1991) 167.

[7] C. Mias, J. P. Webb, R. L. Ferrari, Finite element modelling of electromagnetic waves in doubly and triply periodic structures, IEE Proc.-Optoelectron. 146 (1999) 111.

[8] J. G. Fleming, S. Y. Lin, El-Kady, R. Biswas, K. M. Ho, All-metallic three-dimensional photonic crystals with large infrared bandgap, Nature 417 (2002) 52.

[9] S. G. Johnson, J. D. Joannopoulos, Block-iterative frequency-domain methods for maxwell's equations in a planewave basis, Optics Express 8 (2001) 173.

[10] A. Pletzer, Python & finite elements, Dr. Dobb's Journal 334 (2002) 36.